nature communications

Article

https://doi.org/10.1038/s41467-026-68674-z

Photo-induced selective N-N bond construction via harnessing nitrene release and transfer

Received: 7 August 2025

Accepted: 14 January 2026

Published online: 27 January 2026

Check for updates

Mingming Yu[1] ✉, Jing Feng[1,2], Xingyu Wang[3], Xinyuan Xiang[1], Ye Hu[4], Ze-Hua Wang[1], Ze-Feng Xu[1], Jialong Jie[4] ✉, Hongmei Su[4] ✉, Hao Tang[3] ✉ & Chuan-Ying Li[1,2] ✉

Nitrogen incorporation is fundamental in organic synthesis for functional materials, pharmaceuticals, and agrochemicals. While C–N bond formation has gained great progress, N-N bond construction remains challenging: existing methods rely on prefunctionalized precursors, and direct coupling is hindered by narrow substrate scope and poor reactivity control. Although transition-metal-catalyzed nitrene strategies exhibit high efficacy for intermolecular N–H insertion, nitrene-mediated N–N coupling under metal-free conditions has rarely been explored. Herein, we report a broadly applicable sulfilimine-based approach for selective N–N coupling. By leveraging sulfilimines as nitrene precursors, we achieve controlled release of highly reactive nitrene intermediates, enabling intermolecular N-N coupling with amines. This strategy provides an alternative pathway for nitrene-mediated N-H insertion reaction over conventional methods, providing a streamlined route for constructing complex N–N-containing architectures.

Nitrogen incorporation is fundamental in organic synthesis for functional materials, pharmaceuticals, and agrochemicals. While significant progress has been made in this process via C-N bond construction, forming nitrogen–nitrogen (N-N) bonds, which are prevalent motifs in diverse natural products, remains challenging (Fig. 1a)[1–6]. Current strategies for constructing N-N-containing scaffolds predominantly rely on the modification of N-N or N = N precursors, such as hydrazine and diazo compounds[7–9]. However, direct N-N coupling holds the promise of a more streamlined and convergent synthetic approach, offering enhanced retrosynthetic flexibility and the potential for the rapid assembly of complex N-N-containing architectures. The inherent high electronegativity of nitrogen pose a significant barrier to non-polar N–N bond construction[4,10–13], particularly in intermolecular reactions[12–14]. Although several elegant N-N cross-coupling methods have been developed, which employed oxidative, reductive or radical cross-coupling pathways to form hydrazines, these pioneer methods were often restricted to the synthesis of specific classes of compounds, such as N-N linked bicarbazoles and tetra-aryl substituted hydrazines[11,15–19]. A promising route for intermolecular N-N coupling is electron-deficient nitrene transfer to amines. Transition-metal-catalyzed nitrene insertion, using Ag and Rh[20,21], Fe/Ir/Cu[22,23],and Ni catalysts[24] to regulate the reactivity of nitrenes (Fig. 1b), performs well for sulfonyl/acetyl nitrenes, pave the path to the diversified N-N coupling products. Building on these advancements, we sought to explore whether nitrene-mediated N-N coupling could be successfully achieved by selecting appropriate nitrene precursors under metal-catalyst-free condition, thus a potential approach that would enable access to a broader range of hydrazine products.

Photochemistry presents an equally important and complementary approach for the generation of nitrene species and enables some unbelievable transformations[25–34]. In these cases, most of these photochemical reactions are associated with unsaturated bonds or

[1]School of Chemistry and Chemical Engineering, Zhejiang Sci-Tech University, Xiasha West Higher Education District, Hangzhou, China. [2]Keyi College, Zhejiang Sci-Tech University, Shaoxing, China. [3]College of Chemistry and Materials Engineering, Wenzhou University, Wenzhou, China. [4]College of Chemistry, Beijing Normal University, Beijing, China. ✉e-mail: yumm@zstu.edu.cn; jialong@bnu.edu.cn; hongmei@bnu.edu.cn; tanghao@wzu.edu.cn; licy@zstu.edu.cn

https://doi.org/10.1038/s41467-026-68674-z

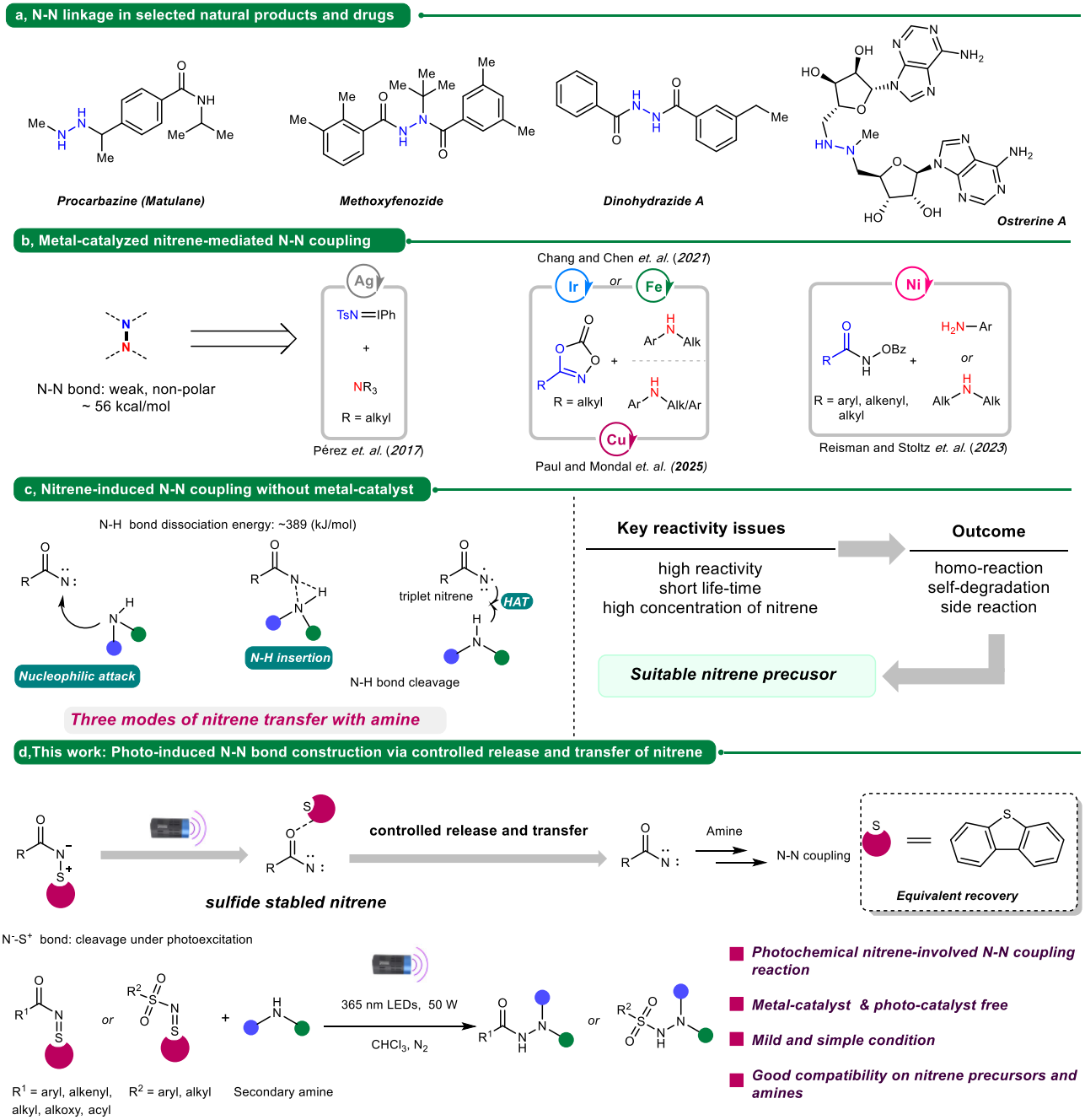

Fig. 1 | Background and our strategy for the nitrene-mediated construction of intermolecular N-N bond. a N-N linkage in selected natural products and drugs (**b**) Metal-catalyzed nitrene-mediated N-N coupling (**c**) Nitrene-induced N-N coupling without metal-catalyst (**d**) This work: Photo-induced N-N bond construction via controlled release and transfer of nitrene.

intramolecular processes. Applying photo-induced nitrene generation to N-N bond construction is still fraught with challenges. Several issues need to be aware of: Firstly, free nitrenes are highly reactive and short-lived species, harsh reaction conditions for their generation often leads to undesired side reactions[21,22,35,36]. Secondly, the selectivity of N-H cleavage is influenced by the spin state of nitrenes, with triplet and singlet nitrenes participating in different reaction pathways. Specifically, singlet nitrenes may be involved in the direct nucleophilic attack process and N-H insertion, while triplet nitrenes undergo hydrogen atom transfer. Thirdly, controlling the concentration of nitrenes is a significant hurdle, as many previous methods involve gas liberation for nitrene generation[37–39], and high nitrene concentrations exacerbate the occurrence of side reactions (Fig. 1c).

Building on previous research into photochemical nitrene-involved amination reactions, we aimed to identify a readily accessible, photoactive nitrene precursor that could achieve the aforementioned N-N coupling. Sulfilimines emerged as a particularly promising candidate: owing to their diverse reactivity profiles and ease of structural modification, these compounds have already found widespread application in amination processes[36–40]. Notably, diarylsulfoneimine—a well-documented member of the sulfilimine family-exhibits intrinsic photochemical activity and has been shown to undergo efficient amination reactions under light-irradiation conditions[28,40–47]. This inherent photochemical activity, coupled with the modular nature of sulfilimine structures, offers two key advantages: first, it facilitates the controlled generation of nitrene

intermediates upon photoexcitation, and second, it allows for the precise tuning of nitrene reactivity through structural modifications of the sulfilimine scaffold. Here, we propose sulfilimines as nitrene precursor, with the potential to pave the way for efficient, metal-free, nitrene-mediated N–N coupling reactions (Fig. 1d).

Results

Condition optimizations

Our investigation commenced by preparing a series of sulfilimines **1a-1**–**1a-4** with the goal to implement N-N bond construction of an aniline moiety with sulfilimines (see Supplementary information Section 2 for the synthesis of these reagents). After screening of conditions, *N*-(5λ^4-dibenzo[*b*,*d*]thiophen-5-ylidene)−4-methylbenzamide **1a-1** showed optimal reactivity in the N-N coupling reaction, for the sulfilimines derived from other diaryl sulfides **3″**–**2**–**3″**–**4** (entries 2-5, Table 1), lower yields were obtained. Subsequently, solvents were tested detailly, when chloroform was chosen as solvent, best outcomes in yield and selectivity were achieved and byproduct 4-methylbenzamide produced using DMSO, CH_3CN and DMF as solvent (entries 6-13, Table 1). Finally, the light parameters were screened, the wave length of light was 365 nm, 50 W turned out to be the best choice (entries 14-16, Table 1). Additionally, under air atmosphere, the target product was obtained in 31% yield (entry 17, Table 1). And further control experiment without light irradiation, the two reaction reactants were remained and no reaction occurred (entry 18, Table 1).

Scope of substrate

With the optimal reaction conditions established, we systematically evaluated the substrate scope of amine reactants in their coupling with N-(5λ^4-dibenzo[*b*,*d*]thiophen-5-ylidene)−4-methylbenzamide (**1a-1**). As illustrated in Fig. 2, N-monosubstituted aniline derivatives efficiently furnished the corresponding N-N coupling products (**3**–**10**) with isolated yields ranging from 50% to 72%, demonstrating slight influence of substituent electronic properties on the phenyl ring. Notably, arylamines bearing five-, six-, or seven-membered ortho-fused aliphatic rings underwent smooth coupling, affording N-N motifs (**11**–**16**) with excellent operational compatibility. Additionally, cyclohexyl and isopropyl anilines were viable substrates, delivering hydrazide molecules (**17**–**19**) in moderate yields.

Next, we assessed the reactivity of aliphatic amines under standard conditions. Remarkably, this method exhibited compatibility with aliphatic amines: various alkylamines, including diethyl-, dipropyl-, isopropyl-, cyclohexyl-, and allylamines (**20**–**24**), provided products in moderate yields with high selectivity. Both ethylbutylamine and methylbenzylamine (**25**–**26**) were successfully incorporated, and cyclic alkylamines demonstrated broad tolerance, yielding hydrazide products (**27**–**30**). Diarylamines also served as viable substrates, although slightly reduced yield was observed for product **31**. The reaction with primary arylamine did not give the desired hydrazide products **32** under our optimized reaction condition, the reaction with aliphatic amine became messy and we could not detect desired hydrazide **33**.

The scope of sulfilimine partners was subsequently explored. A series of N-arylbenzoyl derivatives (**1**) bearing electron-donating or electron-withdrawing substituents afforded corresponding products (**34**–**43**) in good yields (Fig. 3). Polyfluoro-benzoyl, 1-naphthyl, furan-2-yl, and thiophen-2-yl analogs performed comparably, delivering hydrazide products (**44**–**48**) in moderate yields. Extension to non-aromatic acyl groups revealed pivaloyl, (*E*)-but-2-enoyl, and acryloyl derivatives (**49**–**51**) were competent coupling partners. Meanwhile, octadecanoyl-cyclopropyl-, cyclopentyl-, and cyclohexyl-acyl compounds exhibited similar reactivity profiles, furnishing hydrazide products (**52**–**54**). Formate acyl derivatives (**56**–**59**) also engaged smoothly with high reaction efficiency. The scope of sulfonyl-based sulfilimines were further explored: methylsulfonyl-, 1-propanesulfonyl-, cyclopropylsulfonyl-sulfilimines were also candidate substrates, 44-53% yield of target products was furnished (**60**-**62**). Next, aryl-, and 8-quinoline sulfonyl derivatives underwent successful coupling to afford target hydrazides in 44-69 yield (**63**–**70**).

To demonstrate the synthetic utility of this N-N bond coupling strategy in late-stage functionalization, we applied this methodology to a diverse set of bioactive molecules (Fig. 3c). Notable applications included site-selective modification of clinically relevant compounds such as ibuprofen **71**, indomethacin (COX inhibitor) **72**, and probenecid (anti-gout drug) **73**, as well as advanced intermediates like *L*(-)-10-camphorsulfonyl chloride **74** and (-)-camphanic acid **75**. The protocol efficiently introduced nitrogen-based moieties into structurally complex frameworks, including hydro-1H-benzo[*b*]azepine (neuroactive scaffold) and a glycine derivative (**76**), showcasing broad compatibility with heterocyclic systems and chiral centers.

Synthetic applications

To detect the utilization potential of our strategy, a series of synthetic applications were carried out. This method is easy to operate and could be carried at 3 mmol scale with 73% isolated yields (668 mg). In addition, methylation was also smoothly achieved to form the desired product **67** in high yields. Further derivatizations of products exhibited the potential value of such photochemical transformation to synthesize various hydrazines molecules. For example, with Lawesson's reagent, thioacyl hydrazines can be accessible in a direct way. Furthermore, the palladium-catalyzed arylation and amination reaction of **67** pave the pathway towards functionalized hydrazines (Fig. 4).

Mechanistic studies

To gain more details of this photochemical nitrene-mediated N-N coupling reaction, mechanistic studies were carried out to shed light on the process of this transformation. Firstly, TEMPO and BHT were added as additives under the standard reaction, the target product yield of this reaction decreased, which means that the reaction may involve the radical process partially (Fig. 4a). When we used deuterium substrate **2a-D** (98%D) as substrate, **3-D** (66%D) was obtained. To further determined the hydrogen source, the reaction with deuterated methyl aniline (**2a-CD_3**) was performed under standard reaction condition and 22% deuterium incorporation on N-D moiety of **3-CD_3**. These results collectively support the mechanism involving hydrogen atom abstraction from the methyl group of *N*-methylaniline by the generated triplet nitrene (Fig. 4b). Then, the reaction of **1a-1** with alkene containing cyclopropyl groups substrate was carried out, ring-open product was detected by High Resolution Mass Spectrometer (HR-MS) (Fig. 4c), and SPh_2 PPh_3 and cyclohexa-1,4-diene were selected as nitrene-trapping agent, corresponding nitrene insertion adducts were also detected by HR-MS, these results directly verify the generation of free nitrene intermediates. Additionally, electron paramagnetic resonance (EPR) experiments were carried out to capture radical species with the addition of radical scavenger 5,5-Dimethyl-1-pyrrolidine *N*-oxide (DPMO), a weak and messy radical signal was observed using sulfilimine **1a-1** under 1-h 365 nm LED irradiation (Supplementary Fig. 5), confirming the triplet nitrene may generated. Further spin-trapping experiments suggest that the triplet nitrene generated from light-irradiation of sulfilimine **1a-1**, reacts with morpholine to yield the corresponding nitrogen-centered radical ($g = 2.0072$, $A_{N1} = 14.3$ G, $A_H = 17.1$ G, $A_{N2} = 1.8$ G), these results indicated possibility of triplet nitrene-mediated hydrogen atom transfer (HAT) process (Fig. 4d).

Theoretically, the production of the nitrene intermediate requires the excitation of sulfilimine, which means that continuous light irradiation should be necessary. The light on/off experiments verified this viewpoint (Fig. 5a). Subsequently, the UV-Vis absorption spectra reveal that all tested sulfilimines display a strong absorption band below

https://doi.org/10.1038/s41467-026-68674-z

Table 1 | Optimization of the photo-induced N-N coupling reaction

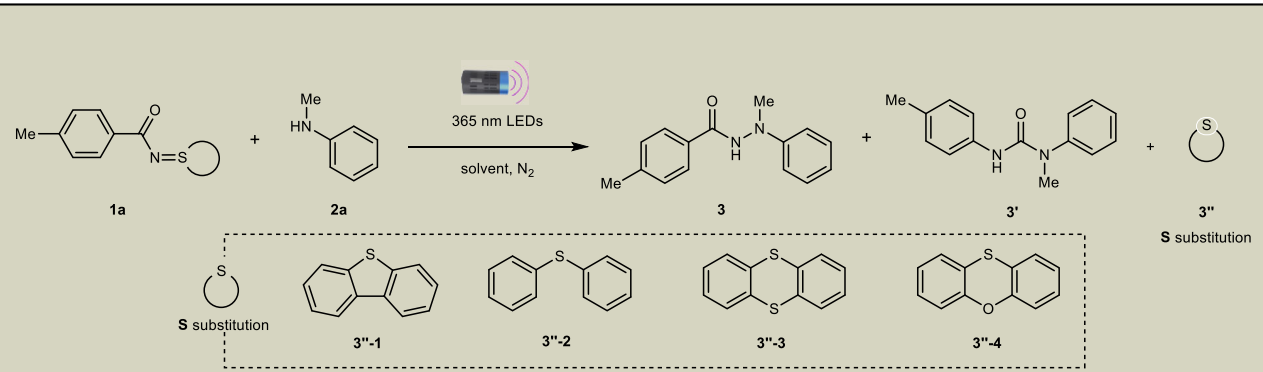

Entry[a]	S Substitution	Solvent	Light	Yield of 3 (%)	Selectivity of 3: 3'[c]
1	**3''-1**	$CHCl_3$	365 nm, 50 W	72	6.5: 1
2	**3''-2**	$CHCl_3$	365 nm, 50 W	21	> 20: 1
3	**3''-3**	$CHCl_3$	365 nm, 50 W	Trace	-
4	**3''-4**	$CHCl_3$	365 nm, 50 W	23	> 20: 1
5[d]	**3''-1**	DCE	365 nm, 50 W	61	2.9: 1
6[d]	**3''-1**	DCM	365 nm, 50 W	25	1.9: 1
7[d]	**3''-1**	EA	365 nm, 50 W	21	5.3: 1
8[d]	**3''-1**	THF	365 nm, 50 W	22	> 20: 1
9[d]	**3''-1**	1,4-Dioxane	365 nm, 50 W	15	1.9: 1
10[d]	**3''-1**	CH_3CN	365 nm, 50 W	Trace	-
11[d]	**3''-1**	DMSO	365 nm, 50 W	Trace	-
12[d]	**3''-1**	DMF	365 nm, 50 W	Trace	-
13	**3''-1**	$CHCl_3$	390 nm, 50 W	40	20: 1
14	**3''-1**	$CHCl_3$	450 nm, 50 W	32	6.4: 1
15	**3''-1**	$CHCl_3$	365 nm, 30 W	30	1.1: 1
16	**3''-1**	$CHCl_3$	365 nm, 100 W	53	3.5: 1
17	**3''-1**	$CHCl_3$	Under air atmosphere	31	1.6: 1
18	**3''-1**	$CHCl_3$	No light irradiation	-	-

a standard conditions: **1a** (0.2 mmol), **2a** (2.0 equiv.), $CHCl_3$ (2 mL), N_2, 365 nm LEDs, 24 h. **b** Yields of isolated products. **c** selectivity of **3**: **3'** were determined by the isolated yields. **d 2a** (1.2 equiv.). *DCE* 1,2-dichloroethane, *DCM* dichloromethane, *EA* ethyl acetate, *THF* tetrahydrofuran, *DMSO* dimethyl sulfoxide, *DMF N, N*-dimethylformamide.

https://doi.org/10.1038/s41467-026-68674-z

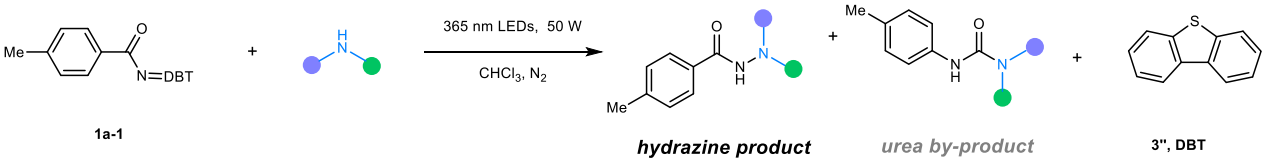

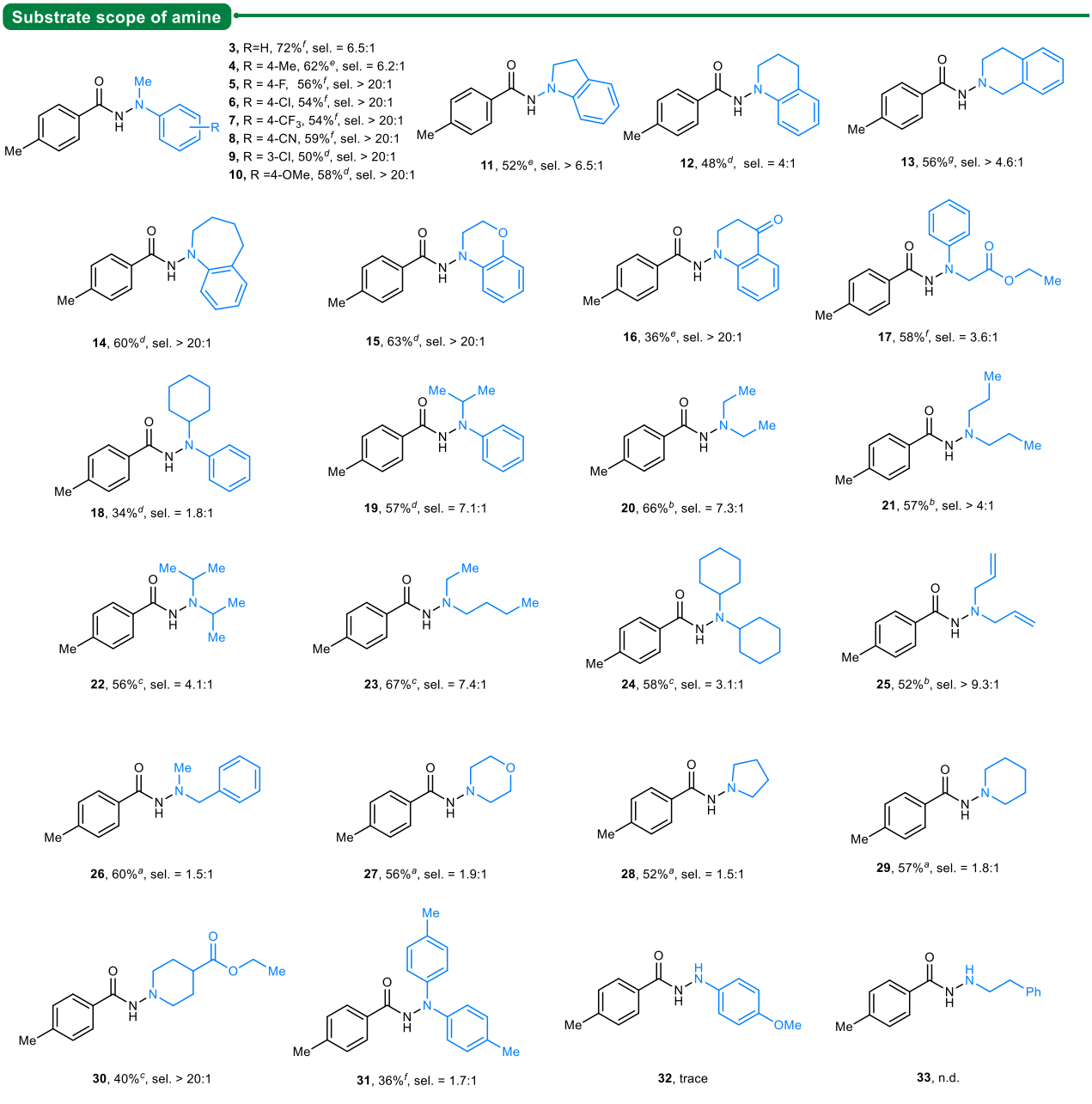

Fig. 2 | Substrate scope of amine. Reaction conditions: **1a-1** (0.2 mmol), amines (2.0 equiv.), $CHCl_3$ (2 mL), N_2, 365 nm LEDs, 24 h. All yields are isolated yields. Selectivity refers to the ratio of hydrazine product/urea by-product. [a]12 h, [b]14 h, [c]16 h, [d]20 h, [e]22 h, [f]24 h, [g]18 h.

360 nm, where absorbance intensifies with decreasing wavelength. What's more, a prominent absorption tail is observed in the range of ca. 360 - 500 nm (Fig. 5b and Supplementary Fig. 2), this is the reason why this strategy is also efficient under blue light (Table 1, entry 14). The UV-Vis absorption spectra showed no significant bathochromic shift for the mixture of **1-16** and **2a** compared to the individual components, and no noticeable absorbance enhancement with the mixture of **1-16** and **2a**, indicating there are no intermolecular interactions involving two starting materials (Fig. 5b). The Stern-Volmer quenching study further illustrated that amine substrate **2a** could effectively quench the excited sulfilimine substrate **1-16** (Fig. 5d). Cyclic voltammetry experiments were carried to gain more details, sulfilimine molecule **1a-1** showed one irreversible reduction peak (E_p = -1.48 V *vs* Ag/AgCl) which refers to the S-N bond cleavage (Fig. 5c). And a reversible reduction peak ($E_{p/2}$ = -2.48 V *vs* Ag/AgCl) was observed which refers to the redox process of dibenzo[*b*,*d*]thiophene (DBT). These CV results indicated that **1a-1** showed remarkable reactivity (Fig. 5c).

https://doi.org/10.1038/s41467-026-68674-z

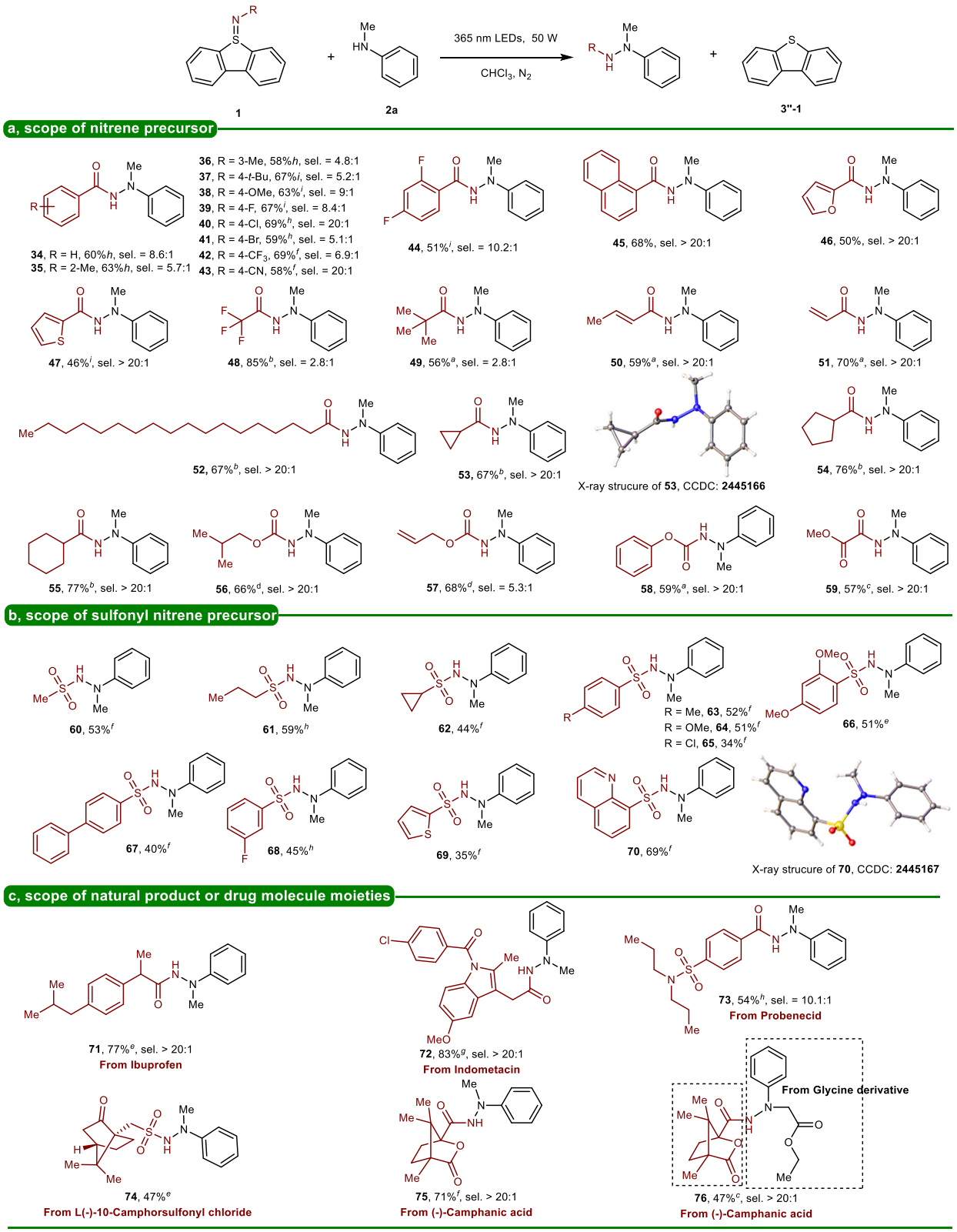

Fig. 3 | Substrate scope of sulfilimine. a scope of nitrene precursor. **b**, scope of sulfonyl nitrene precursor. **c**, scope of natural product or drug molecule moieties. Reaction conditions: sulfilimines (0.2 mmol), amines (2.0 equiv.), $CHCl_3$ (2 mL), N_2, 365 nm LEDs, 24 h. All yields are isolated yields. Selectivity refers to the ratio of hydrazine product/urea by-product. [a]12 h, [b]14 h, [c]15 h, [d]16 h, [e]18 h, [f]20 h, [g]22 h, [h]24 h, [i]26 h.

To elucidate the transient species driving this transformation, we employed time-resolved absorption (ns-TA) spectroscopy. We selected a 355 nm laser to selectively photoexcite the sulfilimine, closely mimicking the 365 nm irradiation used synthetically. Upon excitation of sulfilimine **1-16** in $CHCl_3$, a broad transient absorption signal (360–500 nm) centered at ca. 450 nm forms immediately (Fig. 5e). This initial feature evolves rapidly: the 450 nm band decays within 1 μs, concurrent with intensity growth in the 360–420 nm region over 10 μs

https://doi.org/10.1038/s41467-026-68674-z

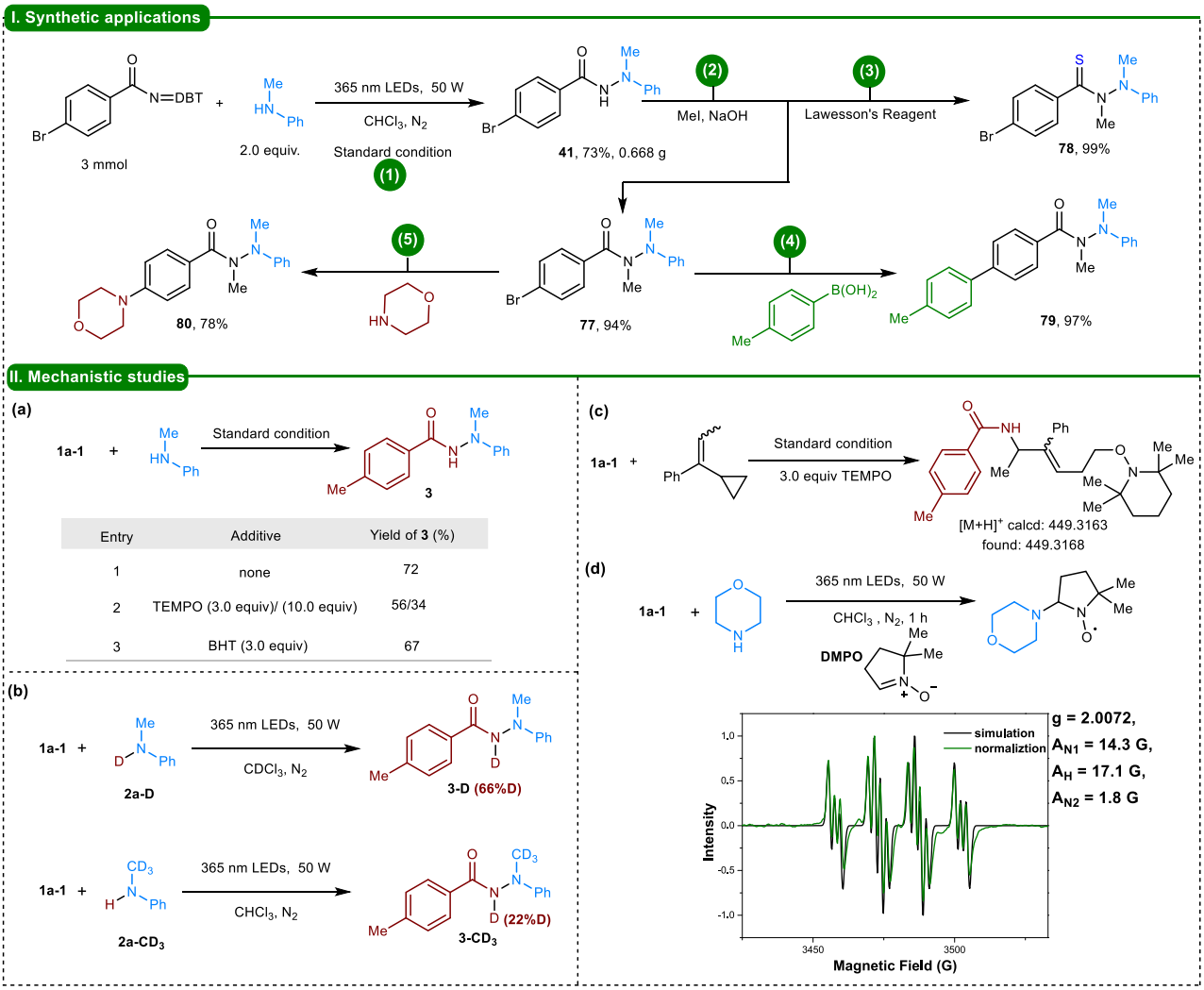

Fig. 4 | Synthetic applications and mechanistic studies. I. Synthetic applications. **1**, 3-mmol scale experiment under standard condition. **2**, MeI, NaOH. **3**, Lawesson's Reagent (1.1 equiv.), Toluene, N_2, reflux, 7 h; **4**, 4-Methylphenylboronic acid (2.0 equiv.), $Pd(PPh_3)_4$ (5 mol%), NaOH (5 equiv.), 1,4-dioxane/H_2O = 5:1, N_2, 100 °C, 8 h; **5**, Morpholine (1.5 equiv.), $Pd(OAc)_2$ (3 mol%), Xantphos (10 mol%), Cs_2CO_3 (1.4 equiv.). **II. Mechanistic studies.** **a** Radical inhibition experiment. **b** Deuterium experiment. **c** Radical ring-open experiment. **d** Electron paramagnetic resonance (EPR) experiment.

timescale. Drawing on literature regarding acylnitrene precursors[48], we assign these phases to sequential nitrene intermediates. The short-lived species around 450 nm is assigned to the triplet acylnitrene. Kinetic analysis reveals its decay is a first-order process sensitive to molecular oxygen (τ = 312 ns under air vs. τ = 1194 ns under deoxygenated conditions), but unaffected by methanol (Fig. 5f and Supplementary Fig. 3a-3b). Conversely, the growth at 360–420 nm corresponds to the decay reactions of the singlet acylnitrene, which is the energetic ground state, stabilized by an interaction between the carbonyl oxygen and the hypervalent nitrogen[48–52]. As shown in Supplementary Fig. 3a, kinetic analysis at 370 nm confirms the reaction process of the singlet acylnitrene is insensitive to oxygen but is accelerated by methanol, consistent with the characteristic reactivity of singlet acylnitrenes: their decay is insensitive to molecular oxygen, but their lifetime is significantly shortened by methanol due to a O–H insertion reaction[48].

In the presence of amine **2a**, the kinetics of the triplet nitrene at 450 nm remained unchanged (Fig. 5g). In stark contrast, increasing concentrations of amine **2a** accelerated the decay of the singlet nitrene (Fig. 5h), demonstrating effectively quenching of the singlet species by amine in competition with its intrinsic decay. Similar spectral results were obtained with other sulfilimine and amine substrates (Supplementary Fig. 3 and Supplementary Fig. 4). A kinetic comparison revealed that aromatic amines are more effective quenchers of the singlet acylnitrene than aliphatic amines (Fig. 5i), which may rationalize the higher selectivity observed for N-N coupling with aryl amine substrates. These ns-TA results establish the ground-state singlet acylnitrene as the key reactive intermediate responsible for the productive N–N bond formation. The reaction proceeds via photoexcitation of the sulfilimine, S = N bond cleavage to generate dual-state (singlet and triplet) nitrenes, and subsequent nucleophilic attack of the amine on the singlet nitrene. Besides, the extended lifetime of the triplet nitrene under anaerobic conditions is expected to permit a secondary interaction with the amine, thereby accessing an additional reaction channel. Furthermore, the continuous irradiation employed in the synthetic protocol maintains a non-zero steady-state concentration of triplet nitrenes, which consequently would serve as supplementary intermediates for the overall transformation.

To gain deeper mechanistic insights, density functional theory (DFT) calculations were performed (see Supplementary information Section 6 for more details.). As depicted in Fig. 6, upon photoexcitation at 365 nm, substrate ^{1CS}**1a-1** is promoted to its singlet excited state (^{1CS}**1a-1***). This singlet state undergoes intersystem crossing to generate the triplet state nitrene (^{3}**1a-1**), which undergoes S-N cleavage and

https://doi.org/10.1038/s41467-026-68674-z

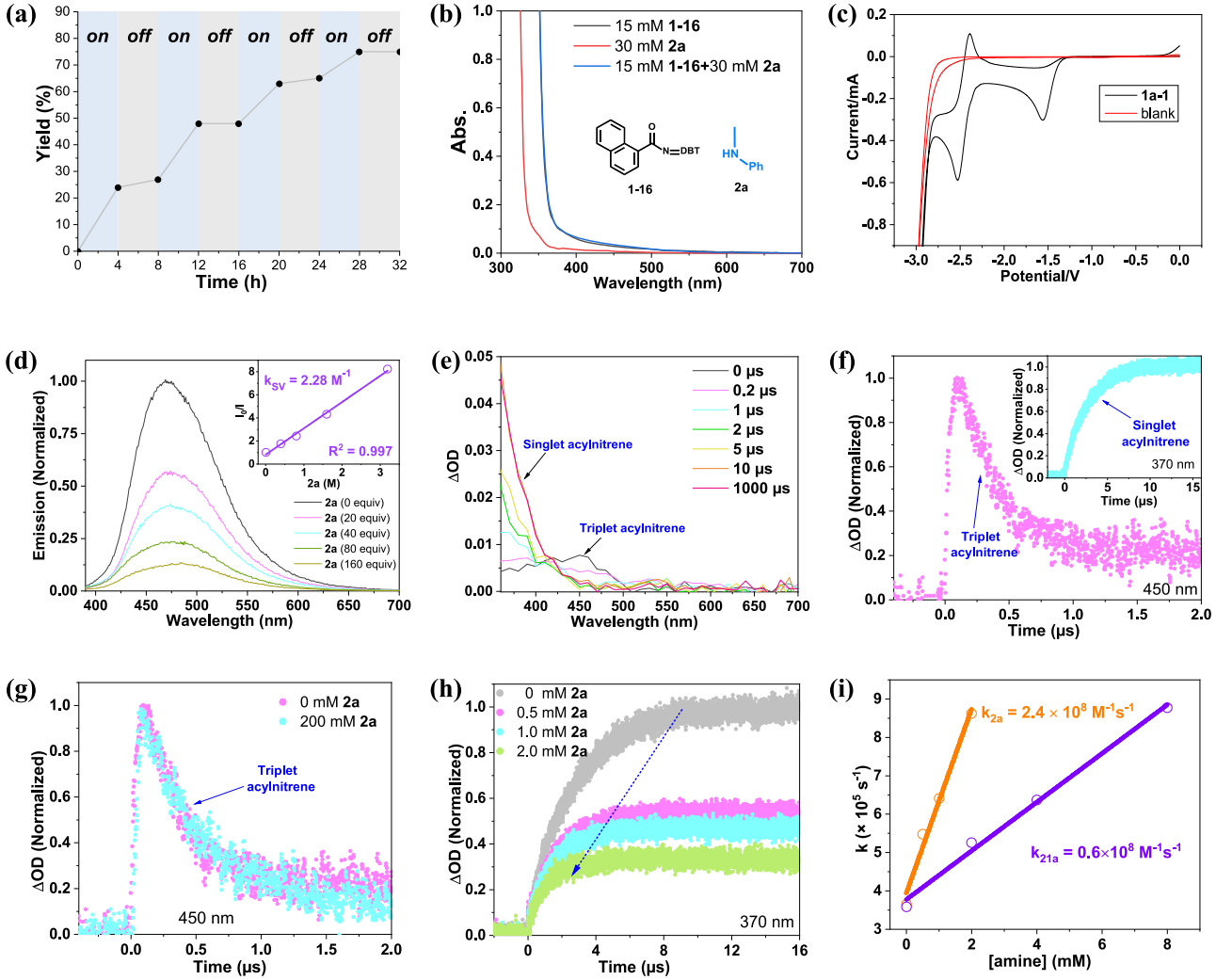

Fig. 5 | Mechanistic studies. a Light/dark on-off experiment; **b** UV-vis absorption spectra of **1-16**, **2a**, and **1-16** + **2a** in $CHCl_3$; **c** Cyclic voltammetry experiment; **d** Steady-state emission spectra for **1-16** at different concentrations of **2a**; Insert: Stern-Volmer plot for **1-16** + **2a**; **e** Transient absorption spectra of **1-16** in $CHCl_3$ after 355 nm laser excitation; **f** Decay traces at 450 nm for triplet acylnitrene of **1-16** and 370 nm for singlet acylnitrene of **1-16**; **g** Decay traces at 450 nm for triplet acylnitrene of **1-16**, and triplet acylnitrene of **1-16** + 200 mM **2a**; **h** Decay traces at 370 nm for singlet acylnitrene of **1-16** at different concentrations of **2a**; **i** Stern-Volmer plots for singlet acylnitrene of **1-16** + **2a** (orange) and singlet acylnitrene of **1-16** + **21a** (purple).

transforms into the singlet closed-shell state ^{1CS}**B1'**, which is susceptible to nucleophilic attack by the lone-pair electrons of *N*-methyl aniline to form ^{1CS}**D**. Notably, an intramolecular hydrogen transfer pathway via the ternary-ring transition state ^{1CS}**TS$_{D\text{-}E}$** was calculated to have a significantly higher energy barrier of 29.3 kcal/mol, highlighting the kinetic preference for the secondary reaction pathway: intermediate ^{1CS}**D** undergoes intramolecular hydrogen transfer through two sequential transition states—^{1CS}**TS$_{D\text{-}D1}$** (involving methyl/hydrogen position exchange) and ^{1CS}**TS$_{D1\text{-}E1}$** (involving 1,4-proton transfer and isomerization)—to generate ^{1CS}**3** (Fig. 6a). An alternative pathway was also explored: computational studies reveal that the selectivity of the nitrene transfer reaction is governed by the controlled release of free nitrene ^{3}**B'**. This spin densities property of the nitrene facilitates the formation of **N:···H − N** non-covalent interactions between ^{3}**B'** and *N*-methyl aniline. Subsequently, a hydrogen atom transfer (HAT) process occurs between ^{3}**B'** and *N*-methyl aniline, yielding intermediate ^{3}**E'** via transition state ^{3}**TS$_{D'\text{-}E'}$** with an energy barrier of 11.5 kcal/mol (Fig. 6b) (see Supplementary Fig. 9 for details of non-covalent interactions (NCI) map of ^{3}**1a-1**, ^{3}C', ^{3}**TS$_{C'\text{-}D'}$** and ^{3}**D'**).

In this study, we report a sulfilimine-mediated approach for selective intermolecular N-N coupling, leveraging photochemical nitrene-involved transformations. This method leverages the inherent properties of sulfilimines to achieve controlled nitrene-mediated reactivity under photochemical activation. The protocol exhibits broad functional group compatibility, facilitating the synthesis of diverse N-N-containing compounds under mild, metal-free conditions. As such, this work provides a complementary tool to the synthetic toolkit for constructing nitrogen-rich architectures, which are relevant to materials science and drug discovery. Mechanistic experiments combined with DFT calculations confirm that the protocol proceeds via dual-state nitrene-mediated N-H bond insertion.

Methods

General procedure for the photo-induced N-N coupling reaction

To a 25 mL Schlenk tube, sulfilimine (0.2 mmol), amine (0.4 mmol) and analytical grade $CHCl_3$ (2 mL) were added under nitrogen atmosphere, then the light (50 W, 365 nm LEDs) was turned on and the reaction mixture was irradiated and stirred at room temperature. After the reaction was completed (monitored by TLC), solvent was removed under vacuum, and the residue was purified by column chromatography on silica gel with a gradient eluent of petroleum ether and ethyl acetate to give products.

https://doi.org/10.1038/s41467-026-68674-z

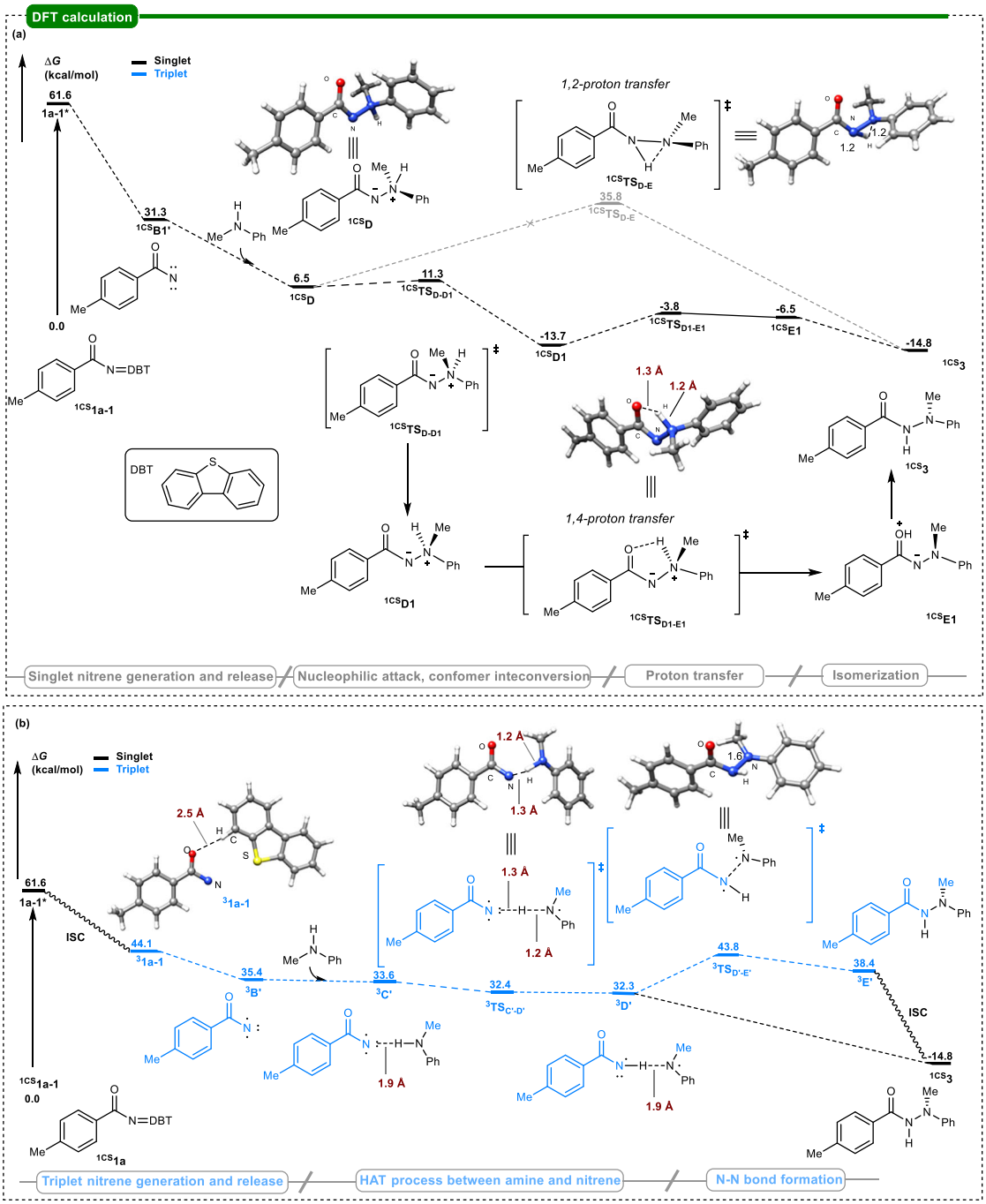

Fig. 6 | DFT calculations. DFT-calculated free energy profiles for the photo-induced N-N coupling reaction. **a** Singlet pathway. **b** Triplet pathway. The relative free energies (*ΔG*, in kcal/mol) are given relative to the separated reactants and were derived from BP86/def2-TZVPP single-point energies incorporating the SMD solvation model (chloroform) and D3 empirical dispersion correction (GD3BJ), combined with thermochemical corrections obtained from B3LYP/def2-SVP frequency calculations.

Data availability

The authors declare that the data supporting the findings of this study are available within the paper and its supplementary information files. Experimental procedures, ^{1}H NMR spectra, ^{13}C NMR spectra, EPR spectra are available in the supplementary information. Source Data are provided with this paper. The X-ray crystallographic coordinates for the structures of compounds **53** and **70** reported in this study have been deposited at the Cambridge Crystallographic Data Centre (CCDC), under deposition numbers 2445166 and 2445167. These data can be obtained free of charge from The Cambridge Crystallographic Data Centre via www.ccdc.cam.ac.uk/data_request/cif. All data are available from the corresponding author upon request. Source data are provided with this paper.

References

1. Blair, L. M. & Sperry, J. Natural products containing a nitrogen–nitrogen bond. *J. Nat. Prod.* **76**, 794–812 (2013).
2. Chen, L., Deng, Z. & Zhao, C. Nitrogen–nitrogen bond formation reactions involved in natural product biosynthesis. *ACS Chem. Biol.* **16**, 559–570 (2021).

3. He, H.-Y., Niikura, H., Du, Y.-L. & Ryan, K. S. Synthetic and biosynthetic routes to nitrogen–nitrogen bonds. *Chem. Soc. Rev.* **51**, 2991–3046 (2022).
4. Tabey, A., Vemuri, P. Y. & Patureau, F. W. Cross-dehydrogenative N–N couplings. *Chem. Sci.* **12**, 14343–14352 (2021).
5. Ahmed, F. S., Helmy, Y. S. & Helmy, W. S. Toxicity and biochemical impact of methoxyfenozide/spinetoram mixture on susceptible and methoxyfenozide-selected strains of Spodoptera littoralis (Lepidoptera: Noctuidae). *Sci. Rep.* **12**, 6974 (2022).
6. Zhou, C. H. & Wang, Y. Recent researches in triazole compounds as medicinal drugs. *Curr. Med. Chem.* **19**, 239–280 (2012).
7. Ragnarsson, U. Synthetic methodology for alkyl substituted hydrazines. *Chem. Soc. Rev.* **30**, 205–213 (2001).
8. Jiang, Y.-S. et al. Photoinduced difunctionalization of diazenes enabled by N–N radical coupling. *Org. Lett.* **25**, 6671–6676 (2023).
9. Zhao, W. E., Fan Yang, J. X. & Zeng, X. I. Advances on the synthesis of N-N bonds. *Chin. J. Org. Chem.* **42**, 1336–1345 (2022).
10. Schmidt, M. W., Truong, P. N. & Gordon, M. S. pi-Bond strengths in the second and third periods. *J. Am. Chem. Soc.* **109**, 5217–5227 (1987).
11. Li, G., Miller, S. P. & Radosevich, A. T. P^{III}/P^{V}=O-Catalyzed intermolecular N–N Bond formation: cross-selective reductive coupling of nitroarenes and anilines. *J. Am. Chem. Soc.* **143**, 14464–14469 (2021).
12. Diccianni, J. B., Hu, C. & Diao, T. N–N nond forming reductive elimination via a mixed-valent nickel(II)–nickel(III) intermediate. *Angew. Chem. Int. Ed.* **55**, 7534–7538 (2016).
13. Pearce, A. J. et al. Multicomponent pyrazole synthesis from alkynes, nitriles, and titanium imido complexes via oxidatively induced N–N Bond coupling. *J. Am. Chem. Soc.* **142**, 4390–4399 (2020).
14. Wang, Y.-P., Guo, Z.-Z., Qu, J.-P. & Kang, Y.-B. Photocatalytic one-step synthesis of unsymmetrical azines. *Org. Lett.* **27**, 1626–1630 (2025).
15. Rosen, B. R., Werner, E. W., O'Brien, A. G. & Baran, P. S. Total synthesis of Dixiamycin B by electrochemical oxidation. *J. Am. Chem. Soc.* **136**, 5571–5574 (2014).
16. Ryan, M. C., Martinelli, J. R. & Stahl, S. S. Cu-Catalyzed aerobic oxidative N–N coupling of carbazoles and diarylamines including selective cross-coupling. *J. Am. Chem. Soc.* **140**, 9074–9077 (2018).
17. Hu, J.-L., Wu, Y., Gao, Y., Wang, Y. & Wang, P. Recent advances in catalytic nitrogen–nitrogen bond formation reactions. *ACS Catal.* **14**, 5735–5778 (2024).
18. Vemuri, P. Y. & Patureau, F. W. Cross-dehydrogenative N–N coupling of aromatic and aliphatic methoxyamides with benzotriazoles. *Org. Lett.* **23**, 3902–3907 (2021).
19. Tombari, R. J. et al. Calculated oxidation potentials predict reactivity in Baeyer–Mills reactions. *Org. Biomol. Chem.* **19**, 7575–7580 (2021).
20. Maestre, L. et al. Functional-group-tolerant, silver-catalyzed N–N Bond formation by nitrene transfer to amines. *J. Am. Chem. Soc.* **139**, 2216–2223 (2017).
21. Kono, M., Harada, S. & Nemoto, T. Chemoselective intramolecular formal insertion reaction of Rh–nitrenes into an amide bond over C –H insertion. *Chem. –A Eur. J.* **25**, 3119–3124 (2019).
22. Wang, H. et al. Nitrene-mediated intermolecular N–N coupling for efficient synthesis of hydrazides. *Nat. Chem.* **13**, 378–385 (2021).
23. Chakraborty, S. et al. Copper-stabilized nitrene radical in N—N coupling: facile synthesis of hydrazides and pyrazole. *Angew. Chem. Int. Ed.* **64**, e202509056 (2025).
24. Barbor, J. P. et al. Development of a nickel-catalyzed N–N coupling for the synthesis of hydrazides. *J. Am. Chem. Soc.* **145**, 15071–15077 (2023).
25. Li, F. et al. Photosensitization enables Pauson-Khand–type reactions with nitrenes. *Science* **383**, 498–503 (2024).
26. Empel, C. & Koenigs, R. M. Visible-light-mediated amination reactions via nitrene intermediates. *Chem. Catal.* **2**, 2506–2514 (2022).
27. Yao, M., Chen, G., Zhang, X., Yusuf, A. & Xu, X. Recent advances on light-mediated nitrene transfer reactions: An Emerging Area. *Eur. J. Org. Chem.* **28**, e202401404 (2025).
28. Song, L. et al. An unexpected synthesis of azepinone derivatives through a metal-free photochemical cascade reaction. *Nat. Commun.* **14**, 831 (2023).
29. Tian, X., Song, L. & Hashmi, A. S. K. Synthesis of carbazoles and related heterocycles from sulfilimines by intramolecular C–H aminations. *Angew. Chem. Int. Ed.* **59**, 12342–12346 (2020).
30. Empel, C., Pham, Q. H. & Koenigs, R. M. Spin states matter—from fundamentals toward synthetic methodology development and drug discovery. *Acc. Chem. Res.* **57**, 2717–2727 (2024).
31. Cai, B.-G., Empel, C., Yao, W.-Z., Koenigs, R. M. & Xuan, J. Azoxy compounds—from synthesis to reagents for azoxy group transfer reactions. *Angew. Chem. Int. Ed.* **62**, e202312031 (2023).
32. Mitchell, J. K., Hussain, W. A., Bansode, A. H., O'Connor, R. M. & Parasram, M. Aziridination via nitrogen-atom transfer to olefins from photoexcited azoxy-triazenes. *J. Am. Chem. Soc.* **146**, 9499–9505 (2024).
33. Kobayashi, Y., Masakado, S. & Takemoto, Y. Photoactivated N-acyliminoiodinanes applied to amination: an *ortho*-methoxymethyl group stabilizes reactive precursors. *Angew. Chem. Int. Ed.* **57**, 693–697 (2017).
34. Guo, Y., Pei, C. & Koenigs, R. M. A combined experimental and theoretical study on the reactivity of nitrenes and nitrene radical anions. *Nat. Commun.* **13**, 86 (2022).
35. Lang, K., Torker, S., Wojtas, L. & Zhang, X. P. Asymmetric induction and enantiodivergence in catalytic radical C–H amination via enantiodifferentiative H-atom abstraction and stereoretentive radical substitution. *J. Am. Chem. Soc.* **141**, 12388–12396 (2019).
36. Ju, M. et al. Tunable catalyst-controlled syntheses of β- and γ-amino alcohols enabled by silver-catalysed nitrene transfer. *Nat. Catal.* **2**, 899–908 (2019).
37. Kuijpers, P. F., van der Vlugt, I. J. I., Schneider, S. & de Bruin, B. Nitrene radical intermediates in catalytic synthesis. *Chem. Eur. J.* **23**, 13819–13829 (2017).
38. Noda, H., Tang, X. & Shibasaki, M. Catalyst-controlled chemoselective nitrene transfers. *Helv. Chim. Acta* **104**, e2100140 (2021).
39. Wentrup, C. Carbenes and nitrenes: recent developments in fundamental chemistry. *Angew. Chem. Int. Ed.* **57**, 11508–11521 (2018).
40. Antoni, P. W. et al. Dibenzothiophenesulfilimines: a convenient approach to intermolecular rhodium-catalysed C–H amidation. *Chem. Eur. J.* **26**, 8235–8238 (2020).
41. Tian, X., Song, L. & Hashmi, A. S. K. -Imino gold carbene intermediates from readily accessible sulfilimines: intermolecular access to structural diversity. *Chem. Eur. J.* **26**, 3197–3204 (2020).
42. Tian, X. et al. Sulfilimines as versatile nitrene transfer reagents: facile access to diverse aza-heterocycles. *Angew. Chem. Int. Ed.* **58**, 3589–3593 (2019).
43. Wiezorek, S., Lamers, P. & Bolm, C. Conversion and degradation pathways of sulfoximines. *Chem. Soc. Rev.* **48**, 5408–5423 (2019).
44. Bizet, V., Hendriks, C. M. M. & Bolm, C. Sulfur imidations: access to sulfimides and sulfoximines. *Chem. Soc. Rev.* **44**, 3378–3390 (2015).
45. Morita, H. et al. Generation of nitrene by the photolysis of N-substituted iminodibenzothiophene. *J. Org. Chem.* **73**, 7159–7163 (2008).
46. Yu, T., Jin, Z., Ji, Y., Yang, A. & Jia, P. Photoredox-catalyzed difunctionalization of alkenes with sulfilimines. *Org. Lett.* **26**, 7944–7948 (2024).
47. Desikan, V., Liu, Y., Toscano, J. P. & Jenks, W. S. Photochemistry of N-acetyl-, N-trifluoroacetyl-, N-mesyl-, and N-tosyldibenzothiophene sulfilimines. *J. Org. Chem.* **73**, 4398–4414 (2008).

48. Desikan, V., Liu, Y., Toscano, J. P. & Jenks, W. S. Photochemistry of sulfilimine-based nitrene precursors: generation of both singlet and triplet benzoylnitrene. *J. Org. Chem.* **72**, 6848–6859 (2007).
49. Autrey, T. & Schuster, G. B. Are aroylnitrenes ground-state singlets? photochemistry of beta.-naphthoyl azide. *J. Am. Chem. Soc.* **109**, 5814–5820 (1987).
50. Sigman, M. E., Autrey, T. & Schuster, G. B. Aroylnitrenes with singlet ground states: photochemistry of acetyl-substituted aroyl and aryloxycarbonyl azides. *J. Am. Chem. Soc.* **110**, 4297–4305 (1988).
51. Pritchina, E. A. et al. Matrix isolation, time-resolved IR, and computational study of the photochemistry of benzoyl azide. *Phys. Chem. Chem. Phys.* **5**, 1010–1018 (2003).
52. Liu, J., Mandel, S., Hadad, C. M. & Platz, M. S. A comparison of acetyl- and methoxycarbonylnitrenes by computational methods and a laser flash photolysis study of benzoylnitrene. *J. Org. Chem.* **69**, 8583–8593 (2004).

Acknowledgements

We are grateful for the support of this work by the National Natural Science Foundation of China (22271254 to C.Y.L., 22401256 to M.Y., 22303062 to H.T., 22473014 to J.J., 21933005 to H.S.), the National Key R&D Program of China (2022YFA1505400 to J.J.), the Natural Science Foundation of Zhejiang province (LQN25B020003 to M.Y.) and Science Foundation of Zhejiang Sci-Tech University (ZSTU) (24262196-Y to M.Y.). We also acknowledge Q. Yang (Wuhan University) for assistance with electron paramagnetic resonance (EPR) experiments.

Author contributions

C.Y.L. and M.Y. conceived the work. M.Y., J.F. and Z.F.X. designed the experiments and analysed the data. J.F., X.X. and Z.H.W. performed the synthetic experiments. X.W. and H.T. contributed to the DFT calculation. J.J. and H.S. designed and analysed mechanistic investigations using time-resolved spectroscopy. Y.H. performed time-resolved spectroscopy experiments. M.Y. and C.Y.L. described original manuscript and all authors revised.

Competing interests

The authors declare no competing interests.

Additional information

Supplementary information The online version contains supplementary material available at https://doi.org/10.1038/s41467-026-68674-z.

Correspondence and requests for materials should be addressed to Mingming Yu, Jialong Jie, Hongmei Su, Hao Tang or Chuan-Ying Li.

Peer review information *Nature Communications* thanks Tiezheng Jia and the other anonymous reviewer(s) for their contribution to the peer review of this work. A peer review file is available.